CONTINUOUS WAVELET TRANSFORM AND WAVELET COHERENCE - IMPLEMENTATION AND APPLICATION TO THE DIVERSIFICATION ANALYSIS OF HEDGE FUND RETURNS

Christoph Auth[1]

Warwick Business School
18. September 2013

Abstract

This paper investigates the diversification benefits of hedge funds as an alternative investment class. For this purpose, it carries out a time-frequency analysis. Wavelet squared coherence estimates based on the continuous wavelet transform measure the co-movements of monthly returns from six hedge-fund indices and the S&P500 Composite Index over the period from January 1994 through December 2012. Additionally, the paper compares the results to coherency spectra based on Fourier transforms. For the wavelet analysis, it employs the commonly used Morlet wavelet, as well as the less popular Paul wavelet, and defines a new smoothing operator for wavelet coherence estimates with the latter function. Results show an increased interrelation between hedge funds and stock markets during financial crises in general and the most recent subprime-mortgage crisis in particular. Therefore, diversification benefits attained through hedge-fund investments became less pronounced during the most recent years, especially for long- and medium-term investors. However, Equity Market Neutral and Global Macro funds still provide relatively good diversification gains.

[1] Correspondence to Christoph Auth (mf12ca@mail.wbs.ac.uk).

1. Introduction

Diversification is the principle of reducing portfolio risk, when measured by the variance of the return distribution (Markowitz 1952). This can be achieved by spreading investments across multiple assets. The lower the correlation between individual asset classes, the larger the resulting diversification benefits for a given portfolio. One of the many potential asset classes to investigate in this context are hedge funds. Füss and Kaiser (2007), amongst others, refer to the low correlation hedge-fund returns show with stock and bond returns as one of the reasons for their impressive success over the last two decades.[2] However, academic research seems to be somewhat divided about the suitability of hedge funds for diversification purposes, with slightly more researchers leaning towards a rather uncorrelated return structure when coupled with equities (Kat 2003a).

In order to find further clarification on this matter, time-frequency analysis using wavelets will be applied. Wavelets are finite wave-like functions, with which one can transform time series into a time-frequency representation. Unlike other time-frequency methodologies, wavelet analysis is not dependent on stationarity assumptions (Burrus, Gopinath and Guo 1998). Recently, McCarthy and Orlov (2012) and Graham, Kiviaho and Nikkinen (2013) showed that the continuous wavelet transform and the wavelet coherence specifically can be used in financial applications to determine correlation estimates across different times and frequencies. This is desirable, since different investors can be seen to influence the asset-price series on different scales. Ultimately, wavelet analysis can be used to detect changes in diversification benefits over time and conclusions for both short- and long-term investors can be drawn.

[2] The terms *correlation* and *co-movement* will be used interchangeably in this paper and the use of the word *correlation* does not necessarily refer to the *correlation coefficient.*

In this paper, the continuous wavelet transform (CWT) and squared wavelet coherence (WCO) will be applied to the analysis of co-movements between S&P500 Index returns and six hedge-fund indices representing funds with different investment strategies. The purpose is to extend the existing literature and the underlying theoretical methods used for the investigation on hedge-fund diversification in academic research.

Furthermore, previous analysis of financial co-movements with the CWT and WCO in empirical papers seems to be commonly performed under the same settings.[3] However, it is not always clear, why these settings are chosen. To investigate the effects of deviations, the analysis will be performed with the Paul wavelet in addition to the commonly used Morlet wavelet. Finally, since most of the practical applications use the CWT without any benchmark, the wavelet analysis will be tested critically and compared with other methodologies to check if additional conclusions can be drawn.

2. Literature Review

Two different methodologies will be used to investigate whether or not hedge-fund returns are uncorrelated with equity returns. These contain the coherence of two time series and concepts based on the continuous wavelet transform. The following section intends to define those concepts and gives a first intuitive interpretation. Some of the current literature on hedge-fund diversification analysis will be given as well as applications of the above theoretical concepts to this problem. Where no literature was found directly related to hedge funds, broader financial applications will be stated.

[3] Cf. Torrence and Compo (1998) and Grinsted, Moore and Jevrejeva (2004) for the settings most frequently used in finance.

2.1 Hedge-Fund Diversification

One of the most commonly used concepts for the diversification analysis of hedge funds is the simple correlation coefficient. Brooks and Kat (2002) and Kat (2002) calculate this coefficient for several publicly available hedge-fund and stock indices over the observation period between January 1995 and April 2001. Besides some few hedge-fund indices containing only funds of certain strategies, relatively high correlation coefficients of up to 0.7 are found.

Other related work points out the dependence of these results on the overall market environment. According to Banz and De Planta (2002), low correlation coefficients of hedge fund returns with the S&P500 can be observed in upward-moving equity markets, but an increasing correlation in bear-market scenarios. Amin and Kat (2002) analyse effects on the distribution of mixed stock and bond portfolios, when constantly increasing the proportion invested in hedge funds. For the analysis, they consecutively include randomly drawn funds in their portfolio. On average, increasing the number of hedge funds leads to a reduction in standard deviation as a measure of risk, which can be taken as an indicator of a low level of correlation. The same argument, namely reduction in portfolio variance after including hedge funds and hence low correlations with other assets, can be found in Kat (2003a).[4]

One disadvantage of this concept is that investors are treated to be homogenous with respect to the length of their investments and only one coefficient is calculated over a whole period of time. Consequently, no recommendation can be given for investors with different investment horizons. Because of this and a relatively large number of existing research on this topic, the correlation coefficient will not be included in the analysis of co-movements in this work.

[4] However, the above-mentioned authors point out that the inclusion of hedge funds comes at the expense of higher kurtosis and reduced skewness measures of the portfolio.

2.2 Frequency Analysis of Financial Co-Movements

To be able to distinguish further between investors with respect to the duration of their investments, one can resort to frequency analysis. By making trading decisions, diverse investors can affect the price series on different frequencies (Corsi 2009). As a consequence, asset classes could incorporate diversification gains only for certain types of investors, when avoiding investments at frequencies which are commonly shared across assets.

Fourier transforms can be used to detect such frequency bands, at which two different asset classes move together (cf. James 2011). The idea behind the Fourier transform is that any stationary process in time can be expressed as a sum of weighted sine or cosine functions with varying frequencies (Granger 1966). At each given frequency, this transform represents the resemblance between the analysed process and sine or cosine functions (Bloomfield 2000). To determine co-movements in frequency domain across different time series, the *cross-spectrum* as a function of frequency ω can be computed and is defined as the Fourier transform of the cross-covariance $\gamma_{yx}(h)$ function from the definition above:

$$s_{yx}(\omega) = \frac{1}{2\pi} \sum_{h=-\infty}^{\infty} \gamma_{yx}(h) e^{-i\omega h} = \frac{1}{2\pi} \sum_{h=-\infty}^{\infty} \gamma_{yx}(h)[\cos(\omega h) - i \cdot \sin(\omega h)]$$

(Hamilton 1994, p.270). Comparable to the well-known covariance and correlation coefficients, this concept can be normalised to the *coherency spectrum* or simply *coherence*,

$$c_{xy}(\omega) = \frac{|s_{yx}(\omega)|^2}{s_y(\omega) s_x(\omega)},$$

yielding a correlation coefficient in frequency space with values between 0 and 1 (Box, Jenkins and Reinsel 1994, p. 456). Just as in the definition of the cross-spectrum, $s_x(\omega)$ and $s_y(\omega)$ respectively denote the Fourier transforms of the auto-covariance functions of the processes X_t and Y_t. Both methods contain information about the frequency components of a

time series and measure how closely the two data series move together across certain frequencies. For their numerical estimation, the NAG functions g13ca can be used to calculate the spectrum of a time series followed by g13ce for the coherency spectrum.[5]

Unfortunately, no research focusing on cross-spectral analysis using hedge-fund data has been found. Several papers however, demonstrate the usefulness of frequency analysis for investigating financial time series with the purpose of diversification. Granger and Morgenstern (1970) were among the first to introduce these concepts for the exploration of stock-market prices. Their research on weekly equity indices from exchanges around the world uses averaged coherence values over all frequencies and reveals little or no evidence for co-movements across those markets from 1961 to 1964. However, a rather sceptical outlook is given on the validity of their results in case of financial turmoil.

This final statement is explored further by Hilliard (1979) who analyses the years of 1973 through 1974, including the OPEC oil embargo and finds relatively high co-movements compared to the previous paper. This statement can also be approved by Fischer and Palasvirta (1990), as well as Smith (1999), who investigate in changes of interdependencies of selected equity indices during the pre- and post-crash period of the 1987 Black Monday. Both papers found increased global co-movements across major financial markets over time and in particular during unstable financial environments.

Unfortunately, frequency information is lost when averaging the estimated coherency spectrum over all frequencies and again, implications for different investors are not clear. Additionally, the time series are assumed to be stationary. However, as the above-mentioned papers show, this cannot always be assumed for financial time series since interrelations between markets seem to change over time and periods of financial crisis. It is therefore

[5] The NAG functions can be called using g13ca/nag_tsa_uni_spectrum_lag and g13ca/ nag_tsa_multi_spectrum_bivar.

desirable to use methodologies which are able to localise changes in frequency components over time and are not dependent on distributional assumptions directly. This can be done effectively by the use of wavelets and time-frequency analysis.

2.3 Time-Frequency Analysis and the Wavelet Transform

Time-frequency analysis involves the detection of frequency components at certain time intervals. This can be thought of by specifying a "window" in both time and frequency and determining how closely the signal coincides with a given function of known frequency inside this “lens”.

As Aguiar-Conraria, Azevedo and Soares (2008) show, an efficient time-frequency localisation can be obtained by using short wave-like functions called wavelets instead of sine and cosine functions.[6] Based on a wavelet function of time, $\psi(t)$, the CWT represents a continuous transformation of a signal $x(t)$ into the time-frequency domain. One can find the following theoretical definition,

$$W_x(n,s) = \frac{1}{\sqrt{s}} \int_{-\infty}^{\infty} x(t) \psi^* \left(\frac{t-n}{s} \right) dt, \quad s \in \mathbb{R}^+, n \in \mathbb{R},$$ [7]

with scale and time shift parameters *s* and *n*, as well as a good introduction into this topic, in Blatter (1998). As Figure 1 shows, the parameters *s* and *n* determine, how stretched or compressed (dilation) the wavelet is and where it is localized in time (translation). Given those parameters, the CWT coefficient then determines how closely the dilated and translated wavelet function resembles the analysed signal at given location in time.

[6] Specifically they show that the use of a Morlet wavelet induces an efficient time-frequency localization. This wavelet function will be discussed later in this work.

[7] In this formula, * denotes the complex conjugate of the wavelet function. Also note that up to the later theoretical treatment, scales and frequency will be referred to interchangeably. This is not mathematically correct, however.

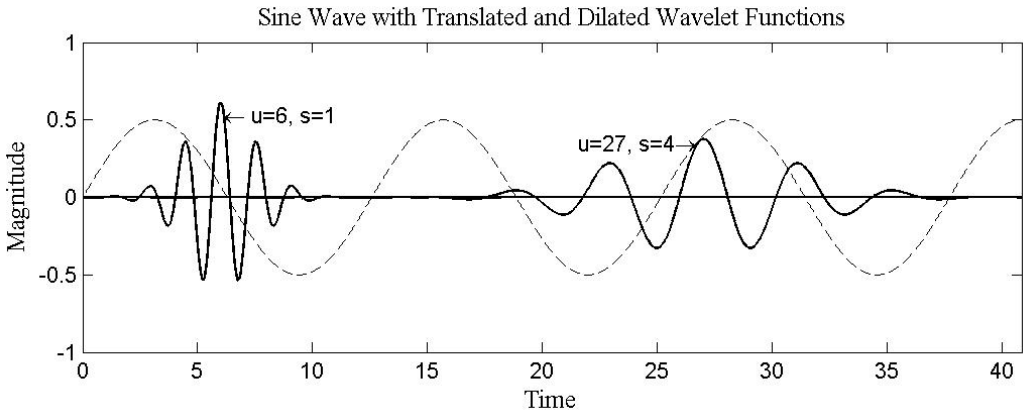

Figure 1: Scaled and shifted real parts of Morlet wavelets (solid) with parameters as shown in the graph alongside a sine wave (dashed).

Based on the calculations of the CWT, the wavelet cross spectrum (WCS) and the wavelet coherence (WCO) can be derived to investigate co-movements of time series, instead of focusing on single time series only.[8] These methods can be seen as estimates of covariance and correlation across different time and frequencies (Liu 1994). The calculation of the wavelet coherence includes a smoothing operation of adjacent time-frequency estimates. It is not straightforward, however, as to what type of smoothing should be implemented and whether or not this should be done in both time and frequency. Torrence and Webster (1999) were the first to give a suggestion for the smoothing with many subsequent papers using their proposal (cf. Grinsted, Moore and Jevrejeva 2004, Bloomfield et al. 2004, Rua and Nunes 2009). Further explanations and comments on this way of smoothing will be given in the methodology section.

2.4 Wavelet Analysis of Financial Co-Movements

The use of methodologies based on the CWT for financial time series is a fairly recent development (cf. McCarthy and Orlov 2012) with relatively limited existing literature, which mainly stems from a small and fixed group of researchers. That wavelet analysis can be

[8] Since it is the focus of this work, a precise definition and more detailed discussion of the wavelet cross-spectrum and the wavelet coherence will be given in the later methodology section.

applied in the study of diversification can be seen in Rua and Nunes (2009), in which interrelations between major developed countries such as Germany and the US are investigated on broad stock-market level as well as reference to economic sub-sectors. Graham, Kiviaho and Nikkinen (2012) extend these tools to the analysis of emerging stock markets across the world and Graham and Nikkinen (2011) specifically compare the Finnish stock market with other markets world-wide. In all of the above papers, squared wavelet coherency results generally indicate a more pronounced co-movement in lower frequencies across markets. This lets the authors conclude that the benefits of diversification are more distinct for short-term investors, as compared to long-term investors. On top of this, markets are observed to become more integrated with each other across all frequencies over time, which is especially apparent when the analysed data sets take the most recent financial crisis into account. This observation is in line with the results yielded by the Fourier techniques.

Graham, Kiviaho and Nikkinen (2013) use the wavelet methodologies and show that commodities offer substantial diversification benefits across all frequencies when mixed with equities. However, they also recognise an increasing co-movement across mainly low frequencies during the last financial crisis. As a result, long-term investors seemed to have had to face less diversification opportunities over the last years, when trying to spread investments across other markets and commodities.

It is unfortunate that all of the above papers use the same setting in terms of wavelet function for their analysis with relatively little explanations. Additionally, only the work of McCarthy and Orlov (2012) uses alternative methodologies such as the cross-spectrum and cross-correlations as a comparative benchmark. Those problems will be addressed in the later empirical analysis.

3. Mathematical Concepts and their Implementation

3.1 Wavelet Requirements

To be applicable for the computation of the CWT, a function of time, $\psi(t)$, has to meet certain criteria. To guarantee a time localisation of frequency components, the function used for the transformation must behave like a window in both time and frequency. For this, it must be well localised in both domains. Consequently, the analysing wavelet has to decrease towards zero relatively quickly in both positive and negative directions of the time domain (Chui 1992). This is contrary to the periodic sinusoidal functions as used for the Fourier transform and it is the reason why the wavelet analysis does not need stationarity assumptions. More theoretically, wavelets have to meet the so-called *admissibility condition*

$$C_\psi = 2\pi \int_{-\infty}^{\infty} \frac{|\Psi(\omega)|^2}{|\omega|} d\omega < \infty$$

to be fully applicable for the calculation of the CWT (Farge 1992, Daubechies 1992). In the above notation, $\Psi(\omega)$ denotes the Fourier transform of the wavelet function and the integral is taken over all frequencies ω. This inequality is necessary for the inversion of the transform back into the time domain and hence to obtain the original time series from the calculated wavelet coefficients (Daubechies 1992). Following Gençay, Selçuk and Whitcher (2002), this condition applies if the wavelet function fulfils the equations

$$\int_{-\infty}^{\infty} \psi(t) dt = 0$$

and

$$\int_{-\infty}^{\infty} |\psi(t)|^2 dt = 1.$$

These two requirements give a more intuitive representation of the conditions on wavelets. In practice, they ensure that the area under the graph above and below the time axis cancels out (first equation) and that the wavelet function has non-zero values (second equation). A wavelet function must therefore oscillate around the time axis and die out quickly in both directions of time.

Two complex wavelet functions will be used for the analysis in this paper. More specifically, the functional form of the Morlet wavelet in time domain can be written as

$$\psi(t) = \pi^{-\frac{1}{4}} \cdot exp\,(i\omega_0 t) exp\,(-t^2/2)$$

with the wavelet parameter ω_0. The corresponding frequency domain representation,

$$\Psi(s\omega) = \pi^{-\frac{1}{4}} \cdot I(\omega) exp\,(-(s\omega - \omega_0)^2/2),$$

has been evaluated at frequencies $s\omega$, since this analytical form will be used for the later implementation of the CWT. $I(\omega)$ denotes the indicator function, which is equal to 1 for $\omega > 0$ and 0 otherwise. Furthermore, the Paul wavelet of order m can be denoted by

$$\psi(t) = \frac{2^m i^m m!}{\sqrt{\pi(2m)!}}(1 - it)^{-(m+1)}$$

in time domain with frequency representation

$$\Psi(s\omega) = \frac{2^m}{\sqrt{m(2m-1)!}} I(\omega)(s\omega)^m\, exp(-s\omega).$$

In the above analytic formulas, *i* denotes the imaginary unit $i = \sqrt{-1}$.

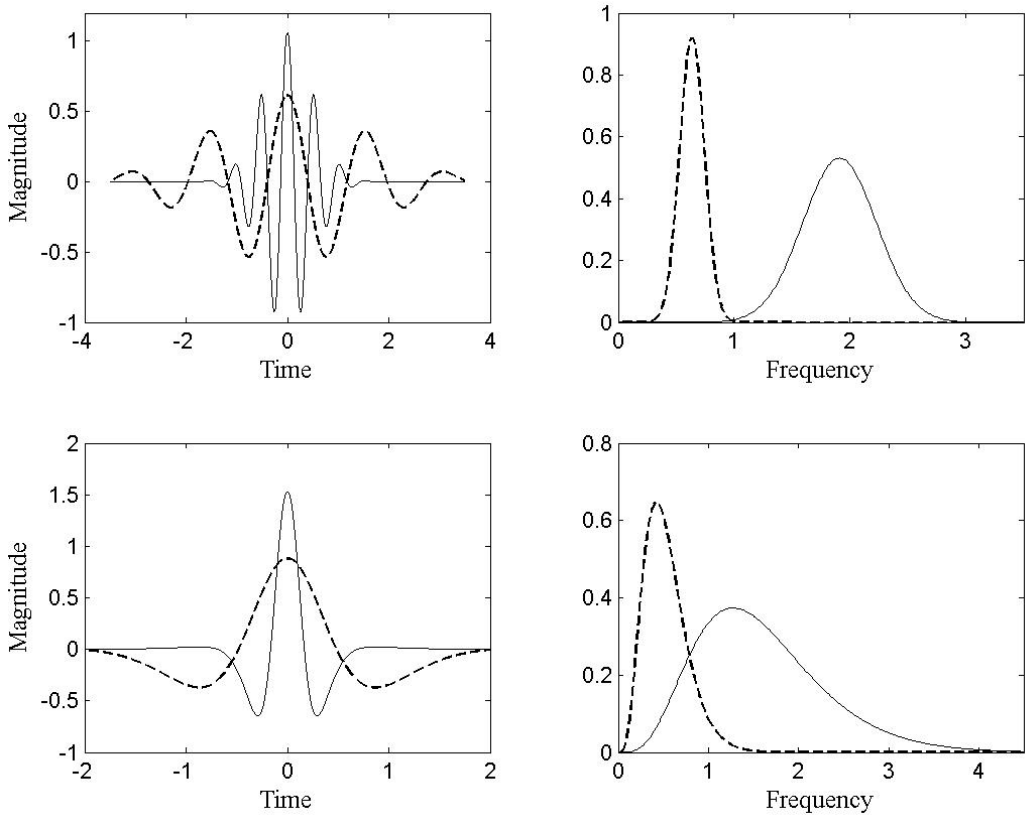

Figure 2: The upper two graphs show the real part of the Morlet wavelet with parameter $\omega_0 = 6$ in the time and frequency domain. Scale values are chosen to be $s = 0.5$ (solid) and $s = 1.5$ (dashed). Lower graphs contain the real part of the Paul wavelet of order $m = 4$ with scale values equivalent to the above.

In line with nearly all of the research undertaken, the parameters of the wavelets in the later analysis will be set to $\omega_0 = 6$ and $m = 4$. In doing so, the Morlet wavelet meets the admissibility condition (Farge 1992). For both of the wavelets this choice of parameters seems to provide a good balance between the resolution in time and frequency (De Moortel, Munday and Hood 2004, Rua and Nunes 2009).

Figure 2 shows the real part of the two wavelets for different scales alongside the functions transformed into Fourier space. As one can see from the graph, increasing the scale parameter increases the time width of a wavelet, but also decreases its frequency range. A Paul wavelet of equal scale is narrower in the time domain, but wider in the frequency domain than the Morlet wavelet. This means that the Paul wavelet can track temporal characteristics more

effectively. However, the Paul wavelet is wider in the frequency domain and hence frequency components will be extracted less accurate.

3.2 Continuous Wavelet Transform - Discrete Representation

As seen in the definition of the CWT, the transform is a convolution of the analysing signal with a dilated and translated wavelet function and assumes a continuous signal as input. However, in empirical applications, data are recorded discretely with time steps denoted by δt.[9] Therefore, a discrete computation of the CWT needs to be performed. At each scale $s \in \mathbb{R}^+$ and for time series data x_n $\{n = 0,1, \dots, N-1\}$ of length *N*, this can be done through

$$W_x(n,s) \approx \sqrt{\frac{\delta t}{s}} \sum_{i=0}^{N-1} x_i \psi^* \left[\frac{(i-n)\delta t}{s}\right],$$

with * denoting the complex conjugate of the wavelet. Here, the continuous version has been approximated by a normalised sum to meet the square integrability requirement as seen in the previous section, and the wavelet function is only evaluated at step sizes δt.

As mentioned earlier, the CWT can be thought of a correlation coefficient between the data and the wavelet function. High wavelet coefficients imply a similar shape of the wavelet function with the time-series data, whereas low coefficients indicate relatively little resemblance at given time-frequency locations. Figures 3 and 4 show examples of CWTs applied to some of the data used in the later empirical analysis. Results for the two Morlet and Paul wavelets are plotted separately. As visible, higher and significant coefficients are coloured red and marked by black contour lines.

[9] For the analysis using the continuous wavelet transform, data will be assumed to be homogeneous and hence, δt is a constant.

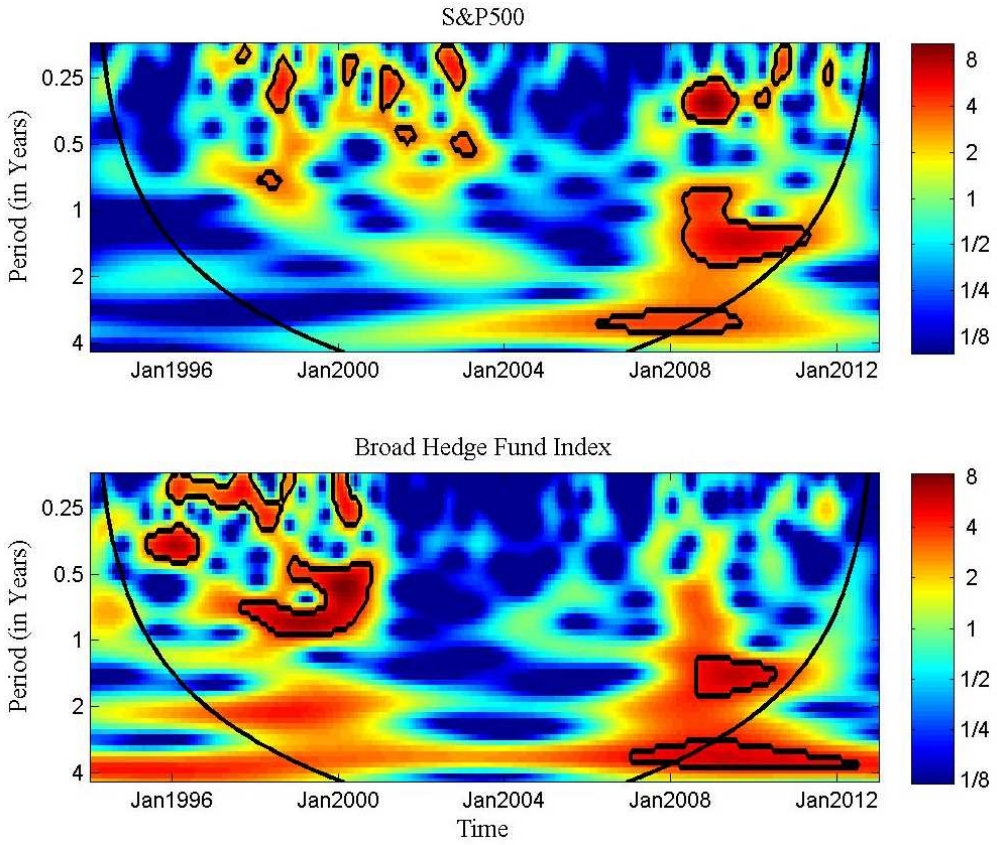

Figure 3: Continuous wavelet transform of the S&P500 and the General Hedge Fund Index as used later in the empirical analysis. The Morlet wavelet was used and the parameters, as explained in the main text, were set to $\omega_0 = 6$, $\delta t = 1/12$, $J = 56$ *and* $\alpha = 12$. *Significant values are obtained from an AR(1) process estimated from the data and are surrounded by a black contour. The black lines towards the beginning and the end of the graphic indicate the possibility of edge effects.*

3.3 The CWT in Fourier Space

For a direct numerical implementation of the CWT using the above discrete definition, the sum needs to be computed for each time value n and scale s separately. Nevertheless, the CWT can be transformed into the frequency-domain, yielding

$$W_x(n,s) = \frac{\sqrt{s}}{2\pi} \int_{-\infty}^{\infty} X(\omega)\Psi^*(s\omega)\, exp(i\omega n)\, d\omega.$$

Again, this integral can be approximated by the formula

$$W_x(n,s) \approx \sqrt{\frac{2\pi s}{\delta t}} \sum_{k=0}^{N-1} \hat{x}_k \, \Psi^*(s\omega_k) exp(i\omega_k n \delta t).$$

Essentially, this formula states that it is sufficient to simply multiply the discrete Fourier transform (DFT),

$$\hat{x}_k = \frac{1}{N} \sum_{n=0}^{N-1} x_n exp\ (-2\pi i k n / N),$$

of the time series by the complex conjugate of the scaled Fourier transform of the wavelet function $\Psi^*(s\omega_k)$. One can calculate the above DFT of the time-series data, by using a fast Fourier transform algorithm. After the multiplication, the obtained results just need to be

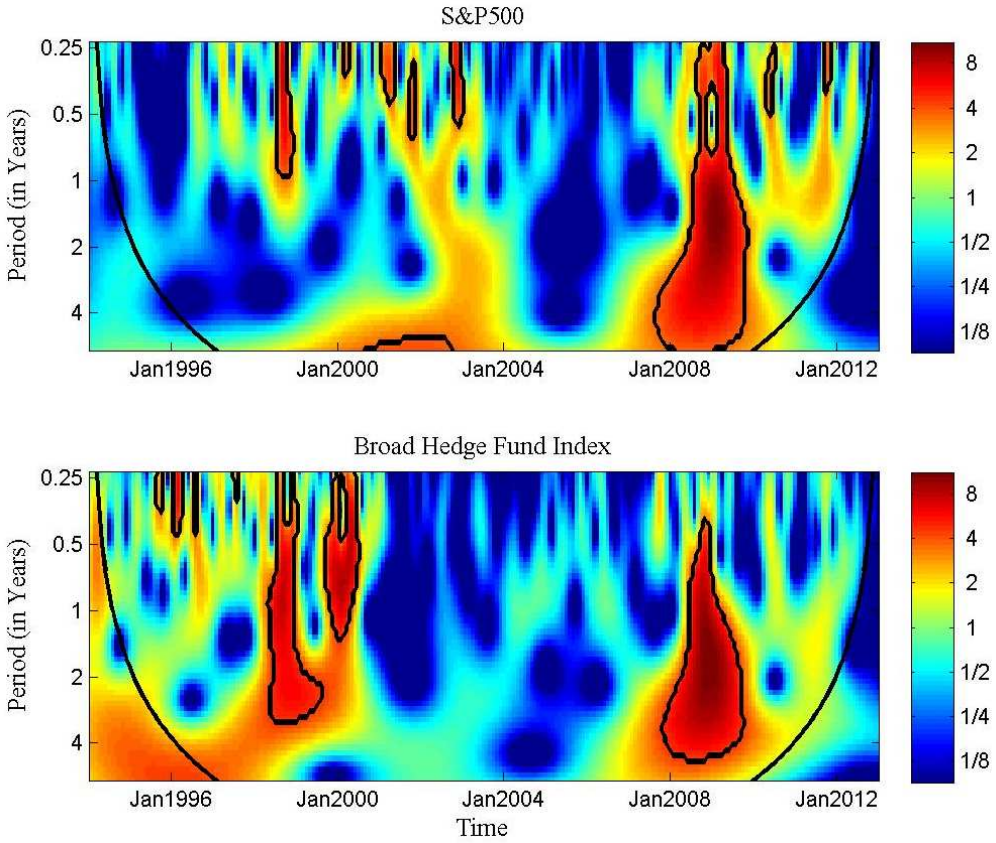

Figure 4: Continuous wavelet transform of the S&P500 and the General Hedge Fund Index with the Paul wavelet. Parameters are set to $m = 4$, $\delta t = 1/12$, $J = 56$ *and* $\alpha = 12$. *Significant values are obtained from an AR(1) process estimated from the data and are surrounded by a black contour. The black lines towards the beginning and the end of the graphic indicate the possibility of edge effects.*

transformed back into the time domain. Both of the above mentioned operations can be performed conveniently with the same NAG function c06pc.[10] As the latter operation can be done for a whole vector using the inverse fast Fourier transform algorithm, wavelet coefficients at given scale values *s* can be computed for all times *n* simultaneously. For an input time series of length *N*, this will lead to a quicker algorithm with $O(N \cdot log(N))$ complexity per scale, compared to a complexity of $O(N^2)$ per scale, when approximating the integral directly in the time domain (Meyers, Kelly and O'Brien 1993).

Additionally, the angular frequencies ω_k for all $k = 0,1, \dots, N-1$ are defined to be

$$\omega_k = \begin{cases} \frac{2\pi k}{N\delta t} & for\ k \leq \frac{N}{2} \\ -\frac{2\pi k}{N\delta t} & for\ k > \frac{N}{2} \end{cases}.$$

The normalisation of the transform by $\sqrt{\frac{2\pi s}{\delta t}}$ again ensures that the wavelet function is square integrable to 1 (Torrence and Compo 1998).

It should be noted that for the calculation of the fast Fourier transform, data of finite length are assumed to be cyclical (Oppenheim, Schafer and Buck 1999). Since most of the financial data do not meet this condition, the algorithm imposes frequency shifts and the wavelet spectrum is distorted at the beginning and end of the observation period, when the data are not pre-processed (Meyers, Kelly and O'Brien 1993). To circumvent this problem, it is possible to pad the time series with zeros at the end.[11] Since the fast Fourier transform algorithm is most efficient if the number of input data is a power of 2, one must add zeros to the time series accordingly.

Besides the performance aspect, another advantage of this algorithm for the use in this paper in particular is that there is no need for transforming the wavelet functions into frequency

[10] The NAG function can be called using c06pc or nag_sum_fft_complex_1d.
[11] For the CWT as calculated in this work, there is no difference if the time series is padded at the end only or at both the beginning and the end.

domain, because the frequency representations $\Psi(s\omega)$ of the two wavelets used herein are known analytically in advance. If this is not the case, additional approximations of the wavelet would need to be performed by a potential algorithm (cf. Jones and Baraniuk 1991).

Finally the CWT will be converted to the normalised *wavelet power spectrum*

$$WPS_x(n,s) = \frac{|W_x(n,s)|^2}{\sigma^2}$$

before the results are plotted, because the wavelet coefficients are complex valued. The normalisation by the variance of the time series will be done to additionally ensure an easier comparison of different wavelet spectra (Torrence and Compo 1998).

3.4 Choice of Scales

Since the CWT needs to be computed discretely, one needs to opt for an appropriate partitioning of the time and scale axes. As empirical data cannot be sampled continuously, the partitioning in time comes naturally with the time series at hand. Nevertheless, it is necessary to select a suitable set of scales. In general, the choice of the scale decomposition for the CWT can be made arbitrarily.[12] However, the set of scales should be chosen to obtain a smooth graphical representation of the wavelet power spectrum. For this purpose, a logarithmic scale grid with base of 2,

$$s_j = 2\delta t \cdot 2^{\frac{j}{\alpha}}, \quad j = 0,1,\dots J,$$

is commonly used (Lau and Weng 1995), where

$$J = \left\lfloor \alpha \cdot log_2\left(\frac{N}{2}\right) \right\rfloor,$$

[12] Note that it is ultimately this choice of scales, which differentiates the continuous wavelet transform from the discrete wavelet transform (Rioul and Duhamel 1992).

determines a default value for the maximum scale value (Torrence and Compo 1998) for which the CWT is computed. Here, $\lfloor \cdot \rfloor$ denotes the floor function. In the above notation, $\alpha \in \mathbb{N}$ defines the number of intermediate scale values computed between two consecutive powers of two. A larger value for α will result in a finer scale decomposition with which one can obtain a smoother picture when graphing the wavelet coefficients. However, one has to keep in mind that an increase in the number of scales comes hand in hand with an increase in the computational effort.

3.5 Conversion from Scales to Fourier Period

So far, CWT calculations are only obtained for a certain set of scales. For most of the wavelet functions however, this is just a simple constant determining the degree of the function's dilation and does not yield any particularly useful practical interpretation. However, one can get at the latter thanks to the Fourier period; it is thus desirable to convert from scales to periods before plotting the wavelet coefficients.

Loosely speaking, the Fourier period of a sinusoidal function – like a sine or cosine function – indicates the time until one cycle passes and the function repeats itself. However, wavelet functions are usually more irregular than simple sinusoidal functions. Nevertheless, the period of a wavelet can be thought of as the maximum period contained in the function.[13] Meyer et al. (1993) propose such a conversion by calculating the CWT of a cosine function of known period and by finding the scale value, at which the wavelet power spectrum is maximised. This indicates the scale coefficient, at which the wavelet correlates the most with the cosine function and hence shares the same period. Fortunately, one can calculate these conversions analytically and obtains them by

[13] Essentially, this is equivalent to finding the peak in the Fourier transform of the wavelet (see figure 4).

$$\lambda_j = \frac{4\pi}{\omega_0 + \sqrt{2 + \omega_0^2}} \cdot s_j$$

for the Morlet wavelet and by

$$\lambda_j = \frac{4\pi}{2m + 1} \cdot s_j$$

for the Paul wavelet with scale index $j = 0,1, \ldots J$.

3.6 Squared Wavelet Coherence

After having obtained the CWT of individual time series, one can use the transform for the investigation of co-movements among two time series. This requires the calculation of the *cross-wavelet transform*,

$$W_{xy}(n,s) = W_x(n,s)W_y^*(n,s),$$

which is a simple multiplication of the CWT of series x_n, with the complex conjugate of the CWT for the time series y_n.[14] This quantity serves as a local covariance between the two series at each time and frequency (Aguiar-Conraria and Soares 2011). Using the cross-wavelet transform, the *squared wavelet coherence* (WCO) can be defined as

$$R_{xy}^2(n,s) = \frac{|\mathfrak{S}(s^{-1} \cdot W_{xy}(n,s))|^2}{\mathfrak{S}(s^{-1} \cdot |W_x(n,s)|^2) \cdot \mathfrak{S}(s^{-1} \cdot |W_y(n,s)|^2)}$$

(Grinsted, Moore and Jevrejeva 2004). Just as one can consider the cross-wavelet transform as a covariance, the wavelet coherence acts as a correlation coefficient between the two time series in time-frequency domain. The operator $\mathfrak{S}(\cdot)$ denotes a smoothing operation of the estimated WCO coefficients first across times and then scales,

$$\mathfrak{S}(\cdot) = \mathfrak{S}_{scale}\big(\mathfrak{S}_{time}(\cdot)\big).$$

[14] For the cross-wavelet transform and ultimately the wavelet coherence, both time series need to have the same length.

Because of the complex nature of the coefficients the wavelet coherence would be equal to 1 for all values n and s without the smoothing operations. Unfortunately, it is not directly clear what window functions one should chose for the smoothing operations. Additionally, no research has been found on the smoothing methodology for the Paul wavelet. Because of this, we will introduce a new concept of smoothing for the complex Paul wavelet in this work. Torrence and Webster (1999) suggest a smoothing method for the Morlet wavelet. However, this proposal is not found to be entirely intuitive, especially for the scale smoothing. Grinsted, Moore and Jevrejeva (2004) apply this method, which uses a simple boxcar function and adopt a constant window size for the smoothing across scales. In contrast, Figure 2 showed that the Fourier transform of the wavelet varies in size with changing scale values and is bell-shaped. Therefore, other window functions for the scale smoothing would have been expected. Nevertheless, in order to obtain comparable results with the work from Grinsted, Moore and Jevrejeva (2004), this idea will also be adopted in this work and extended to the smoothing with the Paul wavelet.

Following Torrence and Webster (1999), smoothing in time, given *s,* is performed by a convolution with the absolute value of the wavelet. For the Morlet function, this can be shown to be a Gaussian function and time smoothing is obtained by

$$\mathfrak{S}_{time}^{M}(W|s) = W * c_1 \exp\left(-t^2/_{2s^2}\right).$$

The constant c_1 is used to normalise the obtained weights of the window, so that they sum up to 1, and $*$ denotes the convolution. Additionally, W acts as a placeholder for the matrix, which eventually gets smoothed. Applying the same method for the Paul wavelet with order *m* (see Appendix A) yields the time-smoothing window

$$\mathfrak{S}_{time}^{P}(W|s) = W * c_1 \left(1 + \frac{t^2}{s^2}\right)^{-\frac{1}{2}(m+1)}.$$

Figure 5 shows the graphs of the time-smoothing windows. Because the Paul wavelet is narrower in the time domain, the smoothing window also proves to be more narrow than the Morlet smoothing window.

To smoothen the value of the transform over scales at given times *t*, one commonly uses

$$\mathfrak{S}_{scale}(W|t) = W * c_2 \Pi\left(\frac{\alpha \delta j_0}{2}\right)$$

(Grinsted, Moore and Jevrejeva 2004). Again, c_2 normalises the filter and $\Pi(\cdot)$ denotes a boxcar-function. The parameter δj_0 is referred to as the scale-decorrelation length and can be derived empirically for each wavelet (Torrence and Compo 1998). This type of scale smoothing will be applied to both wavelets, with a decorrelation length of 0.6 for the Morlet and 1.5 for the Paul wavelet.

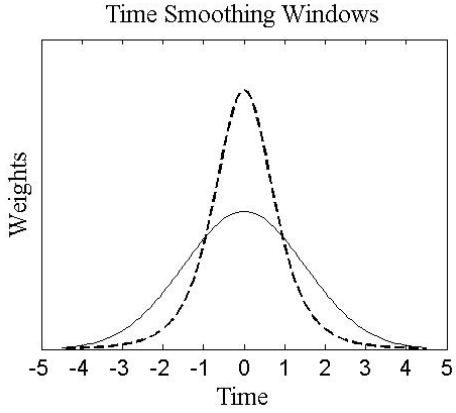

Figure 5: Normalised window functions used for the time smoothing with both Morlet (solid) and Paul wavelet (dashed).The scale value is taken to be 1.5 and coincides with the scale value of the functions in Figure 2.

3.7 Phase Difference

On top of the wavelet coherence, one can obtain information on phase differences when using complex wavelet functions. This is a useful concept, since WCO estimates only yield values between 0 and 1 and one cannot infer the direction of the correlation from the coefficients. However, phase difference estimates can give an indication on whether the common cycles in two time series are positively or negatively correlated and which time series leads ahead of or

lags behind the other one at certain frequency values (Aguiar-Conraria and Soares 2011). To clarify this concept further, note that two harmonic functions may share the same frequency. Nevertheless, they do not need to overlap exactly and can be shifted along the time axis. This shift in the time axis can be measured by the phase difference between the two time series. Phase differences can be calculated by using the imaginary part $\Im(\cdot)$ and real part $\Re(\cdot)$ of the cross-wavelet transform separately:

$$\phi_{xy}(n,s) = tan^{-1}\left(\frac{\Im(W_{xy}(n,s))}{\Re(W_{xy}(n,s))}\right)$$

(Aguiar-Conraria, Azevedo and Soares 2008). The phase difference is expressed in radians and takes the possible values $\phi_{xy}(n,s) \in [-\pi,\pi]$. The obtained results can be categorised and interpreted as follows:

$$\phi_{xy}(n,s) \in \begin{cases} \left(\frac{\pi}{2},\pi\right) & out\ of\ phase, y\ leading \\ \left(0,\frac{\pi}{2}\right) & in\ phase, x\ leading \\ \left(-\frac{\pi}{2},0\right) & in\ phase, y\ leading \\ \left(-\pi,\frac{\pi}{2}\right) & out\ of\ phase, x\ leading \end{cases}$$

In addition to the above categorisation, a value of 0 means that the cycles move together at given periods. A phase difference of π (or $-\pi$) indicates that the cycles of the time series are shifted by 180° – standing for perfectly negative correlation – and y (or x) is leading. For $\phi_{xy}(n,s) = \pm\frac{\pi}{2}$, there is a shift of 90° in the series' cycles and the lead can also be indicated by the sign – positive for x leading, negative for y leading – of the phase difference (McCarthy and Orlov 2012). Without loss of generality, the expressions *in phase* and *out of phase* in this work can be understood respectively as positively and negatively correlated.

The phase information will be plotted on top of the WCO estimates and indicated by the direction of an arrow in terms of the radians. For example, an arrow pointing up and to the right indicates a positive correlation (in phase) between two cycles with x leading.

3.8 Significance Levels

Without further analysis, one has so far only been able to compare the CWT and WCO coefficients to other ones from other transforms. However, relatively large coherence values do not automatically imply significant co-movement between two time series. It is therefore essential to specify and highlight significant time-frequency coefficients. To do so, one can compare the estimated transforms with theoretical coefficients one can obtain from the analysis of time series with known properties.

In this work, Monte Carlo simulations will be applied to create significance intervals. As many financial time series carry a low auto-correlation structure, background signals are restricted to simple AR(1) processes.[15] The implemented method therefore is as follows: Given the AR(1) parameter estimates obtained from the empirical data, we construct two sample paths at each step of the Monte Carlo simulation and compute the WCO. Hereof, we will take only the coherence values for all scales in the middle of the observation period, because these values are affected the least by edge effects. Repeating this procedure *m* times will lead to *m* theoretical values for the squared coherence at each scale.

For the estimation of the AR(1)-coefficient, the NAG function g13ab can be called.[16] Using those estimates for the linear time series model, the NAG functions g05kg and g05ph are then

[15] Note that an AR(1) process includes white noise processes, when the autoregressive parameter is equal to 0.

[16] The NAG function can be called using g13ab or nag_tsa_uni_autocorr. Note, that this function calculates the autocorrelation function of a time series. However, in the case of an AR(1) process, the coefficient is equal to the autocorrelation function at lag 1. Additionally, the function also returns the variance with a single call, which was considered to be very useful in this application.

used to create a random seed and - based on this - a random realisation of the process.[17] With such a sample one can finally obtain confidence intervals. The resulting intervals can then be taken to be valid for every point in time, since the background signals are assumed to be stationary. The expected value of the squared coherence at given scale should therefore not change over time.

4. Empirical Analysis

4.1 Data

Hedge-fund data for the empirical application comes from the Credit Suisse Broad Hedge Fund Index database (www.hedgeindex.com) containing over 9000 funds with at least US$50 million worth of assets under management. Based on this database, Credit Suisse calculates a broad index, representing the hedge-fund industry as a whole as well as several sub-indices containing only funds with certain investment strategies. To expand the investigation from general hedge funds to particular types of funds most suited for the inclusion in equity portfolios, monthly return series data were taken not only from the industry-wide Credit Suisse Hedge Fund Index but also from five Credit Suisse strategy sub-indices (Emerging Markets, Equity Market Neutral, Event Driven, Long/Short Equity and Global Macro).[18] Stock-market data are represented by monthly returns of the S&P500 Composite Index, which can be downloaded from the CRSP database of the Wharton Research Data Service (WRDS). In total, there are 228 monthly data points in the investigated sample, spanning a period of 19 years from January 1994 through December 2012. This sample size includes several financial crises like the burst of the dot-com bubble in 2000 or the subprime mortgage crisis following

[17] The NAG functions can be called using g05kg/nag_rand_init_nonrepeat and g05ph/nag_rand_times_arma, respectively.

[18] To keep the analysis brief, the different types of strategies used in this work will not be explained any further. For a short overview and description of the various hedge-fund strategies cf. Brooks and Kat (2002) or the index descriptions on the Credit Suisse website www.hedgeindex.com.

the years after 2007. Hence, this sample period permits an interesting study of the effects of financial turmoil on the co-movements of hedge-fund and stock-market returns.

4.2 Correlation of Hedge Funds and Equities

Figure 6 shows the results of the coherence estimates between the S&P500 and the broad hedge-fund index in frequency, as well as time-frequency space. Simple coherence estimates reveal surprisingly large values of up to around 0.7, especially for periods bigger than 2 years and for those around ¼ of a year. Contrary to the findings of Füss and Herrmann (2005), this would imply only little diversification benefits for long- and short-term investors.[19]

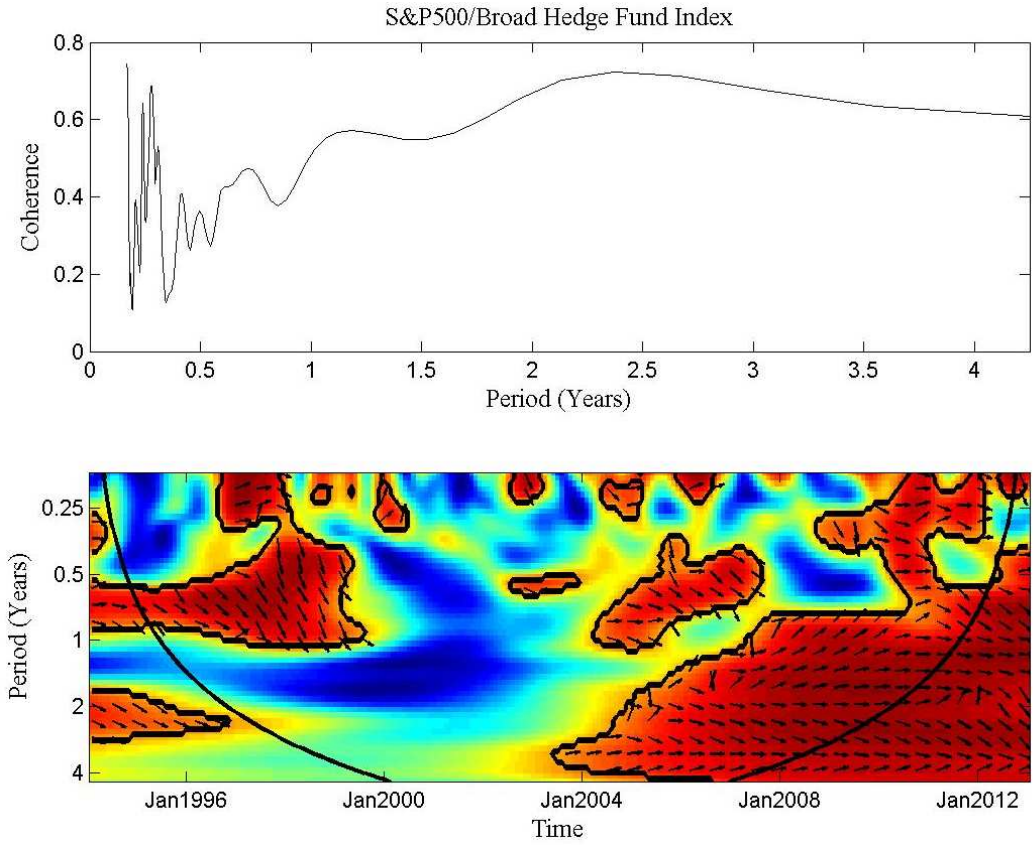

Figure 6: Coherency spectrum and squared wavelet coherence for the S&P500 Index and the broad Hedge Fund Index over the time period from January 1994 through December 2012. The WCO uses the Morlet wavelet and the scale parameters $\alpha = 12$ and $J = 56$. *The number of Monte Carlo simulations is 10.000.*

[19] For this work, we consider it useful to roughly classify investors as short-, medium- and long-term investors. We consider short-term investors to have an investment horizon of about 0-0.5 years, medium-term ones of 0.5 to 2 years and long-term investors of above 2 years. However, these boundaries will only be considered as a rough orientation.

The analysis with wavelets, however, can reveal additional information about the characteristics of co-movements and especially their time location. WCO coefficients show that hedge funds provided good diversification opportunities over the first half of the observation period for long-term investors and for all types of investors following the 3 to 4 years time span after January 2000. In the first half of the observation period, significant correlations can only be found around the year 1997 for investments of approximately 1 year, possibly associated with medium-term consequences of the Asian financial crisis and the associated breakdown of Long-Term Capital Management (LTCM), one of the biggest hedge funds at this time (Edwards 1999). Interestingly, as arrows are pointing downwards and to the right, phase-difference estimates suggest that the hedge-fund index led the stock market across these stated medium-term periods. This suggests that the US-stock market was less affected by direct consequences of the Asian crisis, but indirectly through the breakdown of LTCM.

As the most obvious pattern in the picture, large co-movements between the two indices increased during the second half of the time span and started to spread from high periods to lower periods in early 2004. This increase in the WCO, reflecting the most recent financial crisis, implies only little diversification gains when investing in hedge funds, especially for long- and medium-term investors. Additionally, phase differences seem to have changed over the second half of the observation period, with the two asset classes being in phase and a minor tendency towards a leading US-stock market. Essentially, the Paul wavelet yields the same significant time-frequency areas as can be seen in Figure 9, with slightly better time resolution (cf. for instance the better time localisation of the LTCM breakdown). Again, the broader spectral window of the function stretches significant WCO areas across different periods, which cannot be smoothed away with a window of constant smoothing size.

Overall, as opposed to the coherency spectrum, the wavelet analysis shows an increase in co-movements especially over long- and medium- term periods. For medium- and long-term

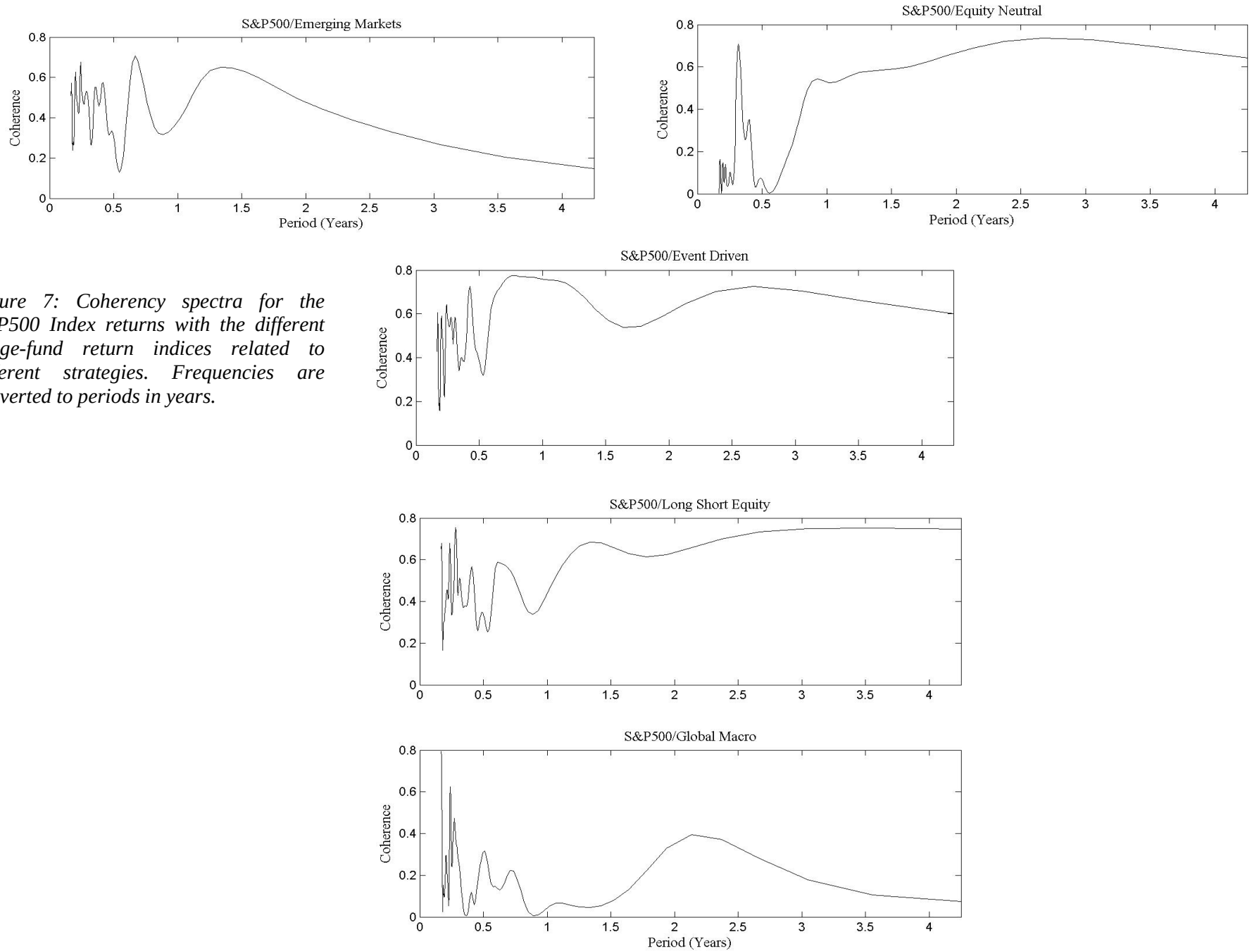

Figure 7: Coherency spectra for the S&P500 Index returns with the different hedge-fund return indices related to different strategies. Frequencies are converted to periods in years.

investors this implies a shift from good to low diversification benefits from the first to the second half of the observation period, which cannot be detected by the normal coherency spectrum. Large correlations over only a shorter period of time seem to highly influence the coherency spectrum and false investment conclusions are likely to be drawn when only looking at the coherence.

The broad hedge-fund index from the Credit Suisse database contains funds with different types of investment strategies. Given this, the interdependencies may be different for particular strategies and diversification gains could be different for investments in funds of specific strategies only.

Coherence estimates for the different hedge-fund strategy indices from Figure 7 impose relatively bad news for long-term investors interested in equity-neutral, event-driven and long/short equity funds. The optimal horizon for hedge-fund investments of any type would be approximately half a year. Based on the coherence estimates, investors could obtain best diversification gains from long-term investments in emerging-market funds and investments in global macro funds for almost any investment horizon.

The wavelet analysis in Figure 8 detects the co-movements across frequencies more precisely in time. All of the strategies presented reveal similar patterns compared to the broad hedge-fund index, with relatively good diversification benefits for long-term investors over the period from January 1994 through January 2004. More distinct, medium term correlations can again be found around the year 1997. Additionally, one can observe a substantial increase in the co-movements between stock markets and hedge funds over time, spreading from longer periods initially, to short-term co-movements.

The wavelet analysis reveals some unexpected patterns in the time-series data when investments in different hedge-fund strategies are considered. In light of especially large areas of significant WCO coefficients during the most recent financial crisis, event-driven and

long/short equity funds seem to offer the least diversification opportunities with a very high proportion of correlated time-frequency areas.

This is rather unsurprising, since both of the funds comprise large amounts of capital invested in equity and therefore are highly affected by unforeseen movements in financial stock markets (Brooks and Kat 2002). Funds investing primarily in emerging-market economies only show a relatively small area of co-movements up to the year 2003. However, the financial crisis of 2008 is likely to have spread to foreign markets, where it tied together US-stock and emerging markets thus diminishing diversification benefits especially for medium term investors (cf. Dooley and Hutchison 2009).

Just as the simple coherence estimates suggested, equity-neutral and global macro funds seem to mix best with equity portfolios, especially over periods of up to 1 year. However, both mentioned funds are affected by the subprime crisis and show an increased co-movement over the second half of the observation period. Nevertheless, this increase in correlation is especially small for global macro funds, which managed to generate returns almost uncorrelated across all times and periods. For hedge fund investors looking for diversification gains, this type of fund therefore seems to be particularly appealing.

Finally, phase differences show that hedge funds and stock-market returns are positively correlated. All of the arrows plotted show values in the range of $\mp\frac{\pi}{2}$, indicated by a direction to either the upper or lower right. However, the lead/lag relationship between the time series changed from hedge funds leading around the year 1997, to stock markets leading or being completely in phase during the most current financial crisis. These results give indications on the relation of the co-movements. Equity markets were likely to be affected indirectly by the Asian crisis through the affiliated breakdown of LTCM. In contrast, stock-market movements had negative effects on the performance of hedge funds during and after the years 2007 and 2008.

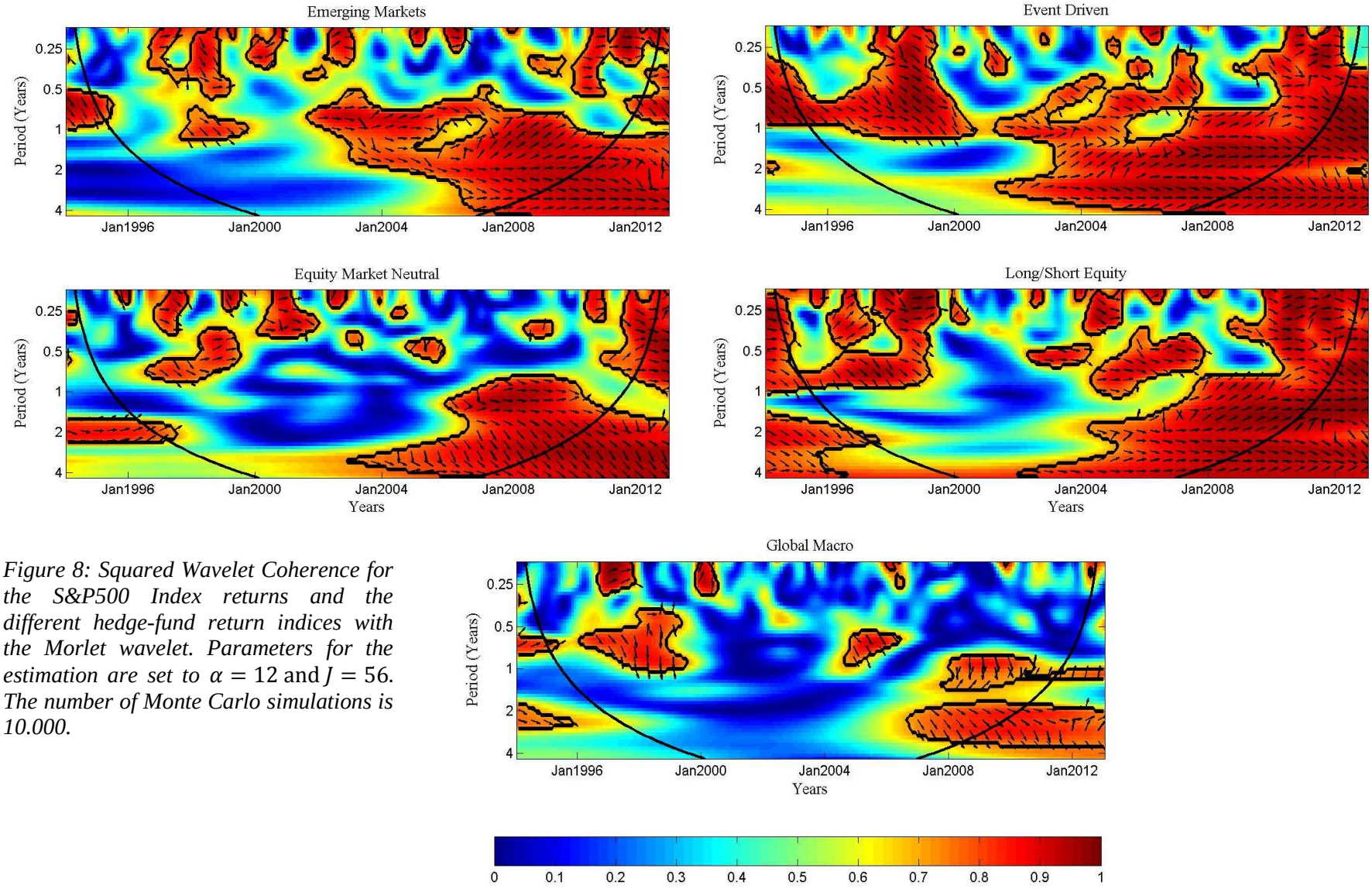

Figure 8: Squared Wavelet Coherence for the S&P500 Index returns and the different hedge-fund return indices with the Morlet wavelet. Parameters for the estimation are set to $\alpha = 12$ *and* $J = 56$*. The number of Monte Carlo simulations is 10.000.*

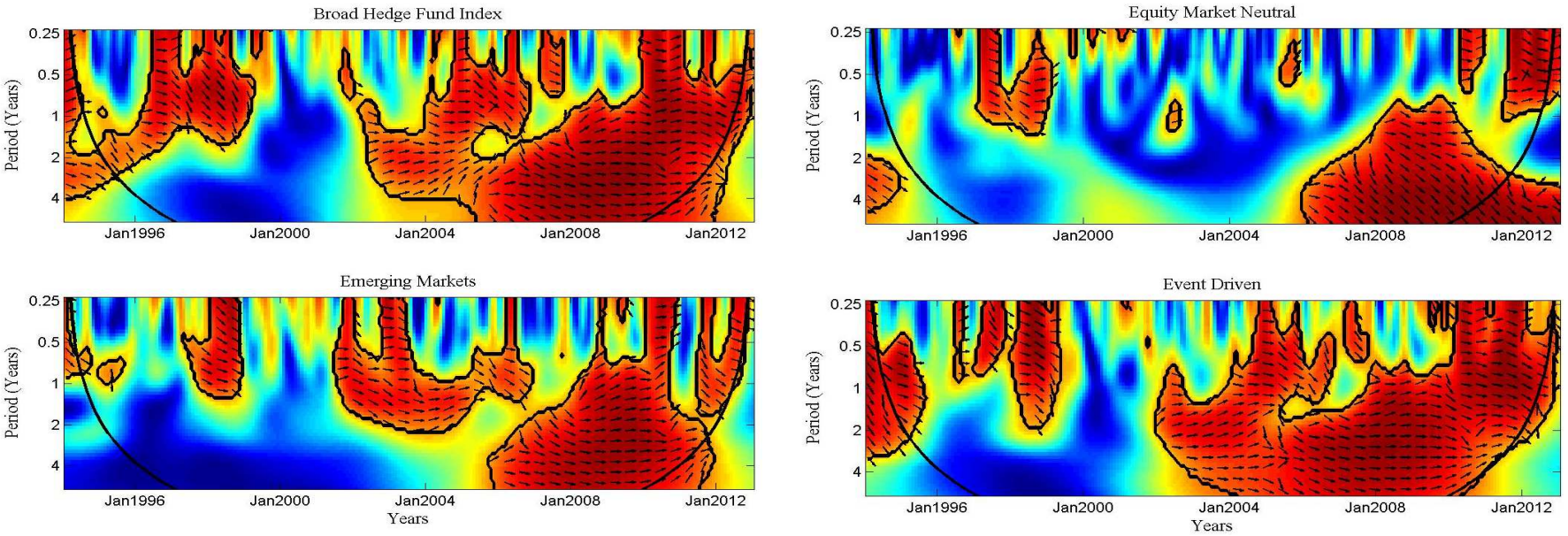

Figure 9: Squared wavelet coherence with the Paul wavelet of order 4. Parameters for the estimation are set to $\alpha = 12$ and $J = 56$. The number of Monte Carlo simulations performed is 10.000.

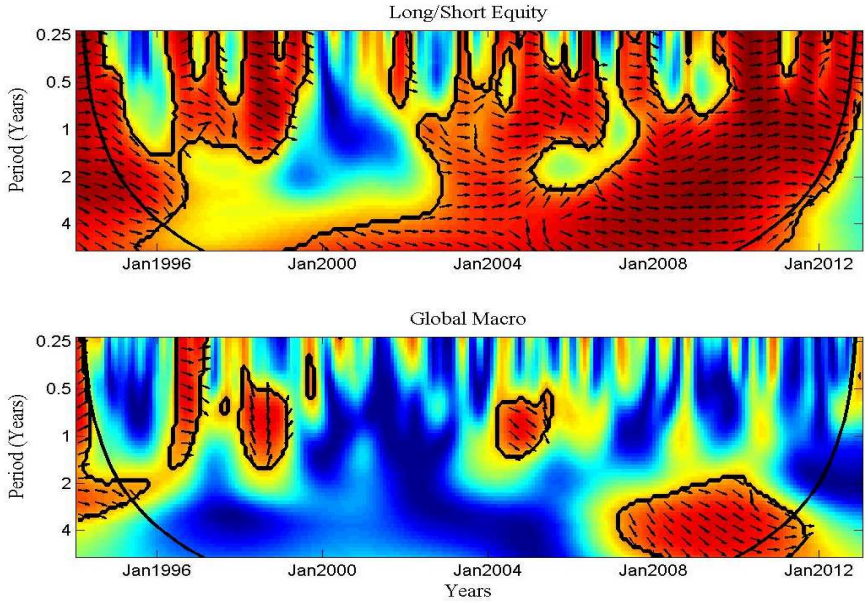

5. Possible Further Work

The purpose of this paper was to investigate if hedge funds can provide uncorrelated returns when compared to general stock-market returns. The underlying question was if the inclusion of hedge funds as an alternative asset class could potentially improve the characteristics of equity portfolios. Regarding hedge funds as an alternative asset class, there are many ways to further expand this work. As an example, one could look at single fund data, as compared to the more general fund strategies, compare the returns to other asset classes like bonds or commodities or simply change the time frequency of the return data. However, consistent with the procedure of Amin and Kat (2002), we believe it would be more interesting to directly assess and evaluate the portfolio characteristics after including hedge funds in existing portfolios. This potential research could then directly quantify the usefulness of the described concepts for portfolio decisions for different types of investors and during various types of financial environments.

More technically and as already stated in the previous chapters, there are multiple factors in the mathematical concept of the squared wavelet coherence, which could be subject to improvement. With this respect, different smoothing operators could be applied to adjust to the changing size of the time-frequency windows implied by the underlying wavelet. Eventually, it would be interesting to see if a more intuitive smoothing would justify the larger computational effort compared to a fixed sized smoothing window.

One of the bigger issues, however, stems from the necessary Monte Carlo Simulations to generate the background spectrum. Because a full matrix of WCO coefficients was estimated for a single vector of background coefficients only, the simulation slows down the calculation of the WCO immensely. Although very difficult to derive, it would be desirable to know analytical formulas of the WCO for the assumed background signal, in which case no

simulation would be necessary. Ge (2008) derived the distribution of the cross-wavelet spectrum and the wavelet coherence, given two Gaussian white-noise processes, as opposed to AR(1) processes used in this paper. However, the obtained results are dependent on the shape of the wavelet function used and are only valid for the Morlet wavelet. Potential further work could be addressed to find a faster and still appropriate way of simulating an assumed background spectrum.

6. Conclusion

This paper explored co-movements between hedge-fund indices of different strategy types and the S&P500 index using concepts based on the continuous wavelet transform. Additional to the Morlet wavelet commonly used in financial applications, it expanded methodologies to the Paul wavelet, for which it introduced a new smoothing approach for the calculation of the squared wavelet coherence. Both wavelets show approximately similar results. However, significant wavelet coherence estimates are dragged over to other frequencies, when using the suggested smoothing operation.

In contrast to the results using Fourier techniques – such as the coherency spectrum – continuous wavelet analysis allows a time localisation of significant co-movements. Making investment decisions by only looking at those concepts could conceal some of the diversification benefits of hedge funds in the beginning of the observation period after 1994, since large co-movements during the most recent financial crisis highly affected the coherency estimates and diversification benefits became less distinct.

In general, hedge-fund and equity returns can be observed to have moved together more closely during the most recent years as compared to the beginning of the sample period starting in 1994. To sum it up, one can say that hedge funds did in fact seem to be a good diversifier for the inclusion in equity portfolios, especially for long- and short-term investors.

These diversification benefits diminished, however, caused by the financial crisis as of 2008 and strong co-movements occurred, spreading from low- to medium-term periods. Nevertheless, when looking at hedge funds of particular investment strategies, equity market neutral and global macro funds reveal the least amount of interrelations with the equity index and hence, can be seen to offer the most diversification benefits amongst all the investigated strategies.

Furthermore, this paper compared the outcomes of the wavelet methodologies with more traditional Fourier based concepts. It is found that an essential factor of the analysis is played by the observation period over which the analysis is performed. As a consequence – as the analysis with the coherency spectrum revealed – the benchmark method seems to be affected, whenever the data bring about a time period of financially unstable markets with large co-movements. Essentially, this is a consequence of the required stationarity assumption, which is unlikely to be fulfilled for financial time series. The analysis with the continuous wavelet transform, however, is not dependent on such restrictive assumptions and is capable of detecting both high and low correlations in relation to time and frequency and hence yields a better tool for the diversification analysis. Given this, it is evident that the analysis by means of squared wavelet coherence estimates provides an extremely useful and powerful tool for analysing diversification and thus for making investment decisions.

6. References

Aguiar-Conraria, L., Azevedo, N. and Soares, M.J. (2008). Using Wavelets to decompose the Time-Frequency Effects of Monetary Policy. *Physica A: Statistical Mechanics and its Applications,* **387**(12), pp. 2863-2878.

Aguiar-Conraria, L. and Soares, M.J. (2011). The Continuous Wavelet Transform: A Primer. *NIPE Working Papers 16/2011, Universidade do Minho.*

Amin, G.S. and Kat, H.M. (2002). Diversification and Yield Enhancement with Hedge Funds. *The Journal of Alternative Investments,* **5**(3), pp. 50-58.

Banz, R. and De Planta, R. (2002). Hedge Funds: All that Glitters is not Gold - Seven Questions for Prospective Investors. *Financial Markets and Portfolio Management,* **16**(3), pp. 316-336.

Blatter, C. (1998). *Wavelets - A Primer.* A K Peters Ltd, Natack, Massachusetts.

Bloomfield, P. (2000). *Fourier Analysis of Time Series: An Introduction.* 2nd Edition, John Wiley & Sons, New York.

Bloomfield, D.S. et al. (2004). Wavelet Phase Coherence Analysis: Application to a Quiet-Sun Magnetic Element. *The Astrophysical Journal,* **617**(1), pp. 623-632.

Box, G.E.P., Jenkins, G.M. and Reinsel, G.C. (1994). *Time Series Analysis: Forecasting and Control.* 3rd Edition, Prentice Hall International, New Jersey.

Brooks, C. and Kat, H.M. (2002). The Statistical Properties of Hedge Fund Index Returns and their Implications for Investors. *The Journal of Alternative Investments,* **5**(2), pp. 26-44.

Burrus, C.S., Gopinath, R.A. and Guo, H. (1998). *Introduction to Wavelets and Wavlet Transforms - A Primer.* Prentice Hall, New Jersey.

Cazelles, B., et al. (2007). Time-dependent Spectral Analysis of Epidemiological Time-Series with Wavelets. *Journal of the Royal Society Interface,* **4**(15), pp. 625-636.

Chui, C.K. (1992). *An Introduction to Wavelets.* Academic Press, London.

Corsi, F. (2009). A simple Approximate Long-Memory Model of Realized Volatility. *Journal of Financial Econometrics,* **7**(2), pp. 174-196.

Daubechies, I. (1992). *Ten Lectures on Wavelets.* CBMS-NSF Lecture Notes Series Nr.61, SIAM.

De Moortel, I., Munday, S.A. and Hood, A.W. (2004). Wavelet Analysis: The effect of varying basic wavelet parameters. *Solar Physics,* **222**(2), pp. 203-228.

Dooley, M. and Hutchison, M (2009). Transmission of the U.S. subprime crisis to emerging markets: Evidence on the decoupling-recoupling hypothesis. *Journal of International Money and Finance,* **28**(8), pp. 1331-1349.

Edwards, F.R. (1999). Hedge Funds and the Collapse of Long-Term Capital Management. *Journal of Economic Perspectives,* **13**(2), pp.189-210.

Farge, M. (1992). Wavelet Transforms and their Applications to Turbulence. *Annual Review of Fluid Mechanics,* **24**, pp. 395-457.

Fischer, K.P. and Palasvirta, A.P. (1990). High Road to a Global Market Place: The International Transmission of Stock Market Fluctuations. *The Financial Review,* **25**(3), pp. 371-394.

Fung, W. and Hsieh, D.A. (2000). Performance Characteristics of Hedge Funds and Commodity Funds: Natural vs. Spurious Biases. *Journal of Financial and Quantitative Analysis*, **35**(3), pp. 291-307.

Füss, R. and Herrmann, F. (2005). Long-Term Interdependence between Hedge Fund Strategy and Stock Market Indices. *Managerial Finance,* **31**(12), pp. 29-45.

Füss, R. and Kaiser, D.G. (2007). The tactical and strategic value of hedge fund strategies: a cointegration approach. *Financial Markets and Portfolio Management,* **21**(4), pp. 425-444.

Gabor, D. (1946). Theory of Communication. *J, IEEE*, **93**(26), pp.429-457.

Ge, Z. (2008). Significance tests for the wavelet cross spectrum and wavelet linear coherence. *Annales Geophysicae,* **26**, pp. 3819-3829.

Gençay, R., Selçuk, F. and Whitcher, B. (2002). *An Introduction to Wavelets and other Filtering Methods in Finance and Economics.* Academic Press, New York.

Gilman, D.L., Fuglister, F.J. and Mitchell, J.M.Jr. (1963). On the Power Spectrum of "Red Noise". *Journal of the Atmospheric Sciences*, **20**(2), pp. 182-184.

Goswami, J.C. and Chan, A.K. (2011). *Fundamentals of Wavelets - Theory, Algorithms and Applications.* 2nd Edition, John Wiley & Sons, New York.

Graham, M., Kiviaho, J. and Nikkinen, J. (2012). Integration of 22 Emerging Stock Markets: A Three-Dimensional Analysis. *Global Finance Journal,* **23**(1), pp. 34-47.

Graham, M., Kiviaho, J. and Nikkinen, J. (2013). Short-term and Long-term Dependencies of the S&P 500 Index and Commodity Prices. *Quantitative Finance,* **13**(4), pp. 583-592.

Graham, M. and Nikkinen, J. (2011). Co-Movement of the Finnish and International Stock Markets: A Wavelet Analysis. *The European Journal of Finance,* **17**(5-6), pp. 409-425.

Granger, C.W.J. (1966). The Typical Spectral Shape of an Economic Variable. *Econometrica,* **34**(1), pp. 150-161.

Granger, C.W.J. and Morgenstern, O. (1970). *Predictability of Stock Market Prices.* Heath-Lexington Books, Lexington, Massachusetts.

Grinsted, A., Moore, J.C. and Jevrejeva, S. (2004). Application of the cross wavelet transform and wavelet coherence to geophysical time series. *Nonlinear Processes in Geophysics,* **11**(5/6), pp. 561-566.

Grossmann, A. and Morlet, J. (1984). Decomposition of Hardy Functions into Square Integrable Wavelets of Constant Shape. *SIAM Journal on Mathematical Analysis,* **15**(4), pp. 723-736.

Hamilton, J.D. (1994). *Time Series Analysis.* Princeton University Press, Princeton, New Jersey.

Hilliard, J.E. (1979). The Relationship between Equity Indices on World Exchanges. *The Journal of Finance,* **34**(1), pp. 103-114.

Hudgins, L., Friehe, C.A. and Mayer, M.E. (1993). Wavelet Transform and Atmospheric Turbulence. *Physical Review Letters,* **71**(20), pp. 3279-3282.

Hubbard, B.B. (1996). *The World According to Wavelets - The Story of a Mathematical Technique in the Making.* A K Peters, Wellesley, Massachusetts.

James, J.F. (2011). *A Student's Guide to Fourier Transforms with Applications in Physics and Engineering.* Cambridge University Press, Cambridge.

Jones, D.L. and Baraniuk, R.G. (1991). Efficient Approximation of Continuous Wavelet Transforms. *Electronic Letters,* **27**(9), pp. 748-750.

Kat, H.M. (2002). Some Facts about Hedge Funds. *World Economics,* **3**(2), pp. 93-123.

Kat, H.M. (2003a). 10 Things that Investors should know about Hedge Funds. *The Journal of Wealth Management,* **5**(4), pp.72-81.

Kat, H.M. (2003b). The Dangers of Using Correlation to Measure Dependence. *The Journal of Alternative Investments.* **6**(2), pp. 54-58.

Lachaux, J.-P., et al. (2002). Estimating the Time-Course of Coherence between Single-Trial Brain Signals: An Introduction to Wavelet Coherence. *Clinical Neurophysiology,* **32**(3), pp. 157-174.

Lau, K.M. and Weng, H. (1995). Climate Signal Detection using Wavelet Transform: How to make a Time Series sing. *Bulletin of the American Meteorological Society,* **76**(12), pp. 2391-2402.

Liu, P.C. (1994). Wavelet Spectrum Analysis and Ocean Wind Waves. In: Foufoula-Georgiou, F. and Kumar, P. *Wavelets in Geophysics*. Academic Press, New York, pp. 151-166.

Mallat, S. (1999). *A Wavelet Tour of Signal Processing.* 2nd Edition, Academic Press, New York.

Markowitz, H. (1952). Portfolio Selection. *The Journal of Finance,* **7**(1), pp. 77-91.

McCarthy, J. and Orlov, A.G. (2012). Time-Frequency Analysis of Crude Oil and S&P 500 Futures Contracts. *Quantitative Finance,* **12**(12), pp. 1893-1908.

Meyers, S.D. Kelly, B.G. and O'Brien, J.J. (1993). An Introduction to Wavelet Analysis in Oceanography and Meteorology: With Applications to the Dispersion of Yanai Waves. *Monthly Weather Review,* **121**(10), pp. 2858-2866.

Morlet, J., et al. (1982a). Wave Propagation and Sampling Theory - Part 1: Complex Signal and Scattering in Multilayered Media. *Geophysics,* **47**(2), pp. 203-221.

Morlet, J., et al. (1982b). Wave Propagation and Sampling Theory - Part 2: Sampling Theory and Complex Waves, *Geophysics,* **47**(2), pp. 222-236.

Nikkinen, J., et al. (2011). Cross-Dynamics of Exchange Rate Expectations: A Wavelet Analysis. *International Journal of Finance and Economics,* **16**(3), pp. 205-217.

Oppenheim, A.V., Schafer, R.W. and Buck, J.R. (1999). *Discrete Time Signal Processing.* 2nd Edition, Prentice Hall, New Jersey.

Plett, M.I. (2007). Transient Detection with Cross Wavelet Transforms and Wavelet Coherence. *IEEE Transactions on Signal Processing,* **55**(5), pp. 1605-1611.

Rioul, O. and Duhamel, P. (1992). Fast Algorithms for Discrete and Continuous Wavelet Transforms. *IEEE Transactions on Information Theory,* **38**(2), pp. 569-586.

Rua, A. and Nunes, L.C. (2009). International Comovement of Stock Market Returns: A Wavelet Analysis. *Journal of Empirical Finance,* **16**(4), pp. 632-639.

Smith, K.L. (1999). Major World Equity Market Interdependence a Decade after the 1987 Crash: Evidence from Cross Spectral Analysis. *Journal of Business Finance & Accounting,* **26**(3)&(4), pp. 365-392.

Torrence, C. and Compo, G.P. (1998). A Practical Guide to Wavelet Analysis. *Bulletin of the American Meteorological Society,* **79**(1), pp. 61-78.

Torrence, C. and Webster, P.J. (1999). Interdecadal Changes in the ENSO-Monsoon System. *Journal of Climate,* **12**, pp. 2679-2690.

Unser, M., Aldroubi, A. and Schiff, S.J. (1994). Fast Implementation of the Continuous Wavelet Transform with Integer Scales. *IEEE Transactions on Signal Processing,* **42**(12), pp. 3519-3523.

Vrhel, M.J. (1997). Rapid Computation of the Continuous Wavelet Transform by Oblique Projections. *IEEE Transactions on Signal Processing,* **45**(4), pp. 891-900.

Wade, R. (1998). The Asian debt-and-development crisis of 1997-?: Causes and consequences. *World Development,* **26**(8), pp.1535-1553.

Zhan, Y., et al. (2006). Detecting time-dependent coherence between non-stationary electrophysiological signals - A combined statistical and time-frequency approach. *Journal of Neuroscience Methods,* **156**(1-2), pp. 322-332.

Appendix A - Theoretical Supplements

A.1 Smoothing with the Paul Wavelet

Smoothing for the Paul wavelet is performed in the same manner as the Morlet smoothing, as detailed in Torrence and Webster (1999). For the time-smoothing window, one calculates the absolute value of the wavelet function scaled by s:

$$\left|\psi\left(\frac{t}{s}\right)\right| = \left|\frac{2^m i^m m!}{\sqrt{\pi(2m)!}}\left(1 - i\frac{t}{s}\right)^{-(m+1)}\right| = \left|\frac{2^m i^m m!}{\sqrt{\pi(2m)!}}\right| \cdot \left|\left(1 - i\frac{t}{s}\right)^{-(m+1)}\right|$$

$$= \left|\frac{2^m i^m m!}{\sqrt{\pi(2m)!}}\right| \cdot \left|\left(1 - i\frac{t}{s}\right)\right|^{-(m+1)}.$$

Note that for even values of m, the first modulus is just a real and positive number. For m being odd, this part yields the modulus of a complex number with real part equal to zero. Using the property of the modulus for complex numbers z as stated in section 7.4, this is just the real part of the complex number itself. In both cases, the first part of the formula is a real and positive number which is ignored, since the window function will be normalised so that the weights sum up to one. The window function for the time smoothing then becomes

$$\left|\psi\left(\frac{t}{s}\right)\right| = \left|\left(1 - i\frac{t}{s}\right)\right|^{-(m+1)} = \left|\left(1 + i\left(-\frac{t}{s}\right)\right)\right|^{-(m+1)} = \left(1 + \frac{t^2}{s^2}\right)^{-\frac{1}{2}(m+1)}$$

Appendix B - MATLAB Code

B.1 Continuous Wavelet Transform

```
%#########################################################################
%####################### Continuous Wavelet Transform ####################
%#########################################################################

function [ wav_coeff ,period ] = nag_cont_wtransform(x,...
                                                wavelet,alpha,J,dt,par)

%*************************************************************************
%   This function calculates the Continuous Wavelet Transform,
%   implemented according to Torrence and Compo (1998).
%
%   INPUT PARAMETERS:
%   x:          Vector of time series data
%   wavelet:    String variable for the choice of the wavelet function. One
%               can choose from two options, either 'morlet' or 'paul'.
%   alpha:      Number of scales between two scales given by powers of 2
%   J:          Maximum scale used for the implementation. If set to 0, the
%               maximum scale from Torrence and Compo (1998) is used.
%   dt:         Time step between observations (e.g. 1/12 for monthly data)
%   par:        Frequency parameter of the Morlet waveler/Order of Paul
%               wavelet
%*************************************************************************
%Chapter 3.4:
%Calculate a scale vector

    N = length(x);
    min_scale = 2*dt;
        if (J == 0)
            J = log2( (N * dt)/ min_scale )*alpha;
            J = floor(J);
        end

    j = 0:1:J;
    scale = (min_scale) * 2.^( j*(1/alpha) );

%*************************************************************************
%Chapter 3.5:
%Conversion from scales to fourier period

    if ( strcmpi(wavelet, 'MORLET') )
        b = 4*pi / ( par + sqrt(2+par^2) );
    elseif ( strcmpi(wavelet, 'PAUL') )
        b = 4*pi / (2*par + 1);
    end
    period = b * scale;

%*************************************************************************
%Chapter 3.3:
%Fourier Transform and angular frequencies

    %Padding the time series with zeros
    x_padded = zeros(2^nextpow2(N),1);
    x_padded(1:N,1) = x;
    N_new = length(x_padded);
```

```
    %Fast Fourier Transform to calculate the CWT in Fourier space using
    %NAG function
    x_padded = complex(x_padded);
    x_transf = nag_sum_fft_complex_1d('F', x_padded);
    Ls = length(scale);

    %Angular Frequency
    number=fix(N_new/2);
    angular =  [0 , (1:1:number), ((number+1):1:N_new-1)*(-1)]';
    angular =  angular .* (2*pi)/(N_new*dt);

    %Calculation of CWT in Fourier space.
    wav_coeff = zeros(Ls, N_new);
    norm=sqrt(2*pi/dt);
        if ( strcmpi(wavelet, 'MORLET') )
            for i=1:Ls
                func = norm * sqrt( scale(i) );
                coeff = func * pi^(-0.25) * ( angular > 0 )...
                    .* exp( -( scale(i)*angular - par ).^2 / 2 );
                wav_coeff(i,:) = ...
                    nag_sum_fft_complex_1d('B', (x_transf.*coeff));
            end
        elseif ( strcmpi(wavelet, 'PAUL') )
            for i=1:Ls
                func = norm * sqrt( scale(i) );
                multipl = func * (2^par) / sqrt( par*factorial(2*par-1) );
                pre_coeff = multipl * ( angular > 0 )...
                    .* ( scale(i)*angular ).^par;
                coeff = pre_coeff .* exp(-scale(i)*angular);
                wav_coeff(i,:) = ...
                    nag_sum_fft_complex_1d('B', (x_transf.*coeff));
            end
        else
            error('Wavelet function does not exist in this application!');
        end

        wav_coeff = wav_coeff(1:Ls,1:N);
```

B.2 Squared Wavelet Coherence

```
%#############################################################################
%######################## SQUARED WAVELET COHERENCE ##########################
%#############################################################################

function [coher,background,period,phase,a,B]= ...
                                    nag_squared_coherence(x,y,wavelet,...
                                     par,dt,alpha,J,number_mc,signif,graph)
%*****************************************************************************
%This Function calculates the wavelet squared coherence alongside
%significance values and phase differences
%
%   INPUT:
%
%   x:          First time series to analyse.
%   y:          Second time series to analyse.
%   wavelet:    Type of wavelet function used, type 'Morlet' for the Morlet
%               wavelet and 'Paul' for the Paul wavelet!
%   par:        Parameter characteriing the wavelet function. Default is
```

```
%               par=6 for the Morlet and par=4 for the Paul wavelet.
%   dt:         Sampling difference of the time series, i.e. 1/12 for
%               monthly data.
%   alpha:      Number of scales in between two consecutive powers of two
%               in the scale vector. Defines, how smooth the calculations
%               for the transform should be.
%   J:          Determines the maximum scale value, which will be
%               calculated. If set to 0, the default max scale of Torrence
%               and Compo (1998) will be used.
%   number_mc:  Number of Monte Carlo simulations for the significance
%               interval.
%   signif:     String variable determining, if significance values and
%               therefore MC simulation needs to be performed. Set to 'yes'
%               if significant values are needed, anything else for no
%               significance checks. If not set to 'yes', the variable
%               number_mc is not valid.
%   graph:      string variable, indicating if a plot of the results needs
%               to be performed or not. Type 'yes' for the plot, anything
%               else for no.
%
%   OUTPUT:
%
%   coher:      Squared Wavelet Coherence Matrix
%   background: Matrix of 0's and 1's regarding significance. A value
%               of 1 stands for a significant value.
%   period:     vector of fourier periods for plotting
%   phase:      matrix full of phase difference estimates
%   a:          Matrices a and B contain information about the location of
%   B:          the phase difference plots on top of the squared wavelet
%               coherence.
%*************************************************************************
%Chapter 3.4:
%Creating a scale vector

    N = length(x);
    min_scale = 2*dt;
    if (J == 0)
        J = log2( (N * dt)/min_scale )*alpha;
        J = floor(J);
    end

    j = 0:1:J;
    scale = (min_scale) * 2.^( j*(1/alpha) );
    N_scale = length(scale);

%*************************************************************************
%Chapter 3.5:
%Conversion from scales to fourier period

   if ( strcmpi(wavelet, 'MORLET') )
        b = 4*pi / ( par + sqrt(2+par^2) );
    elseif ( strcmpi(wavelet, 'PAUL') )
        b = 4*pi / (2*par + 1);
    end
    period = scale .* b;

%*************************************************************************
%Squared Coherence and Phase Difference for the two time series

    [coher,phase] = wave_coher(x,y,wavelet,par,dt,alpha,J,scale);
```

```
%************************************************************************
%Chapter 3.8:
%Monte Carlo Simulation to determine significance levels.

    background = zeros(N_scale,N);
    if ( strcmpi(signif, 'yes') )

    %Estimate the AR(1) coefficients and the variance
    %NAG function g13ab
    [~,sigma1,ar_x,~,~] = nag_tsa_uni_autocorr(x, int64(1));
    [~,sigma2,ar_y,~,~] = nag_tsa_uni_autocorr(y, int64(1));

    %Generate sample paths for the Monte Carlo Estimates
    N_half = floor( N/2 );
    vec = zeros(N_scale,number_mc);

    %Creating the seeds for the following NAG functions
    genid = int64(1);
    subid = int64(1);

        for i=1:number_mc

            %NAG function g05kg
            [state,~] = nag_rand_init_nonrepeat(genid, subid);

            %NAG function g05ph
            [~,~,~,series_1,~] = ...
            nag_rand_times_arma(int64(2),int64(N),0,...
                                ar_x,0,sigma1,zeros(10,1),state);

            %NAG function g05kg
            [state,~] = nag_rand_init_nonrepeat(genid, subid);

            %NAG function g05ph
            [~,~,~,series_2,~] = ...
            nag_rand_times_arma(int64(2),int64(N),0,...
                                ar_y,0,sigma2,zeros(10,1),state);

            %Coherence of the two sample paths
            w_coh = wave_coher(series_1,series_2,...
                                wavelet,par,dt,alpha,J,scale);

            %Coefficients are extracted at half point in time
            vec(:,i) = w_coh(:,N_half);
        end

        %Sort the obtained values with respect to each row (across scales)
        for a=1:N_scale
            vec(a,:) = sort( vec(a,:) );
        end

        %Percentiles for the theoretical spectrum at each scale
        p = 0.05;
        %Number of element in a row, for which 95% of the values lie below
        index = ceil( (1-p) * number_mc );
        theo = zeros(N_scale,1);
        theo(:,1) = vec(:,index);

        for n=1:N
            background(:,n) = theo;
```

```
        end
        background = ( coher > background );
    end

%*********************************************************************
%Introducing matrices for the phase plot.

    t = (1:N).*dt;

    A = ones(N_scale,N);
    B = ones(N_scale,N);
    for k=1:N_scale
        %adjusted to the axis of the coherence plot
        A(k,:)=t;
    end
    for m=1:N
        %adjusted to the axis of the coherence plot
        B(:,m)=log2(period)';
    end

    a = NaN(N_scale,N);
    N_arrow = floor(N/45);
    N_Ls = floor(N_scale/18);

    %Only show arrows at certain positions
    a(1:N_Ls:end,1:N_arrow:end)=A(1:N_Ls:end,1:N_arrow:end);

    if ( strcmpi(signif, 'yes') )
        a(background==0) = NaN;
    end

    %Normalized phase arrows
    C = cos(phase);
    D = sin(phase);
    norm_arrow = sqrt(C.^2 + D.^2);
    C = (C ./ (norm_arrow));
    D = (D ./ (norm_arrow));

%*********************************************************************
%Plotting commands

    if ( strcmpi(graph, 'yes') )

    Yticks = 2.^(fix(log2(min(period))):fix(log2(max(period))));

    imagesc(t,log2(period),coher);
        set(gca,'clim',[0 1]);
        colorbar;
        set(gca,'YLim',log2([min(period),max(period)]), ...
            'YDir','reverse', 'layer','top', ...
            'YTick',log2(Yticks(:)), ...
            'YTickLabel',num2str(Yticks'), ...
            'layer','top')
        ylabel('Period')
        hold on
    if any(background(:))
        contour(t,log2(period),background,'Color','k');
    end
    quiver(a,B,C,D,N_arrow/2,'k','LineWidth',1);
        hold off
```

```
    end

end
%*************************************************************************

%#########################################################################
%################### Wavelet Squared Coherence ###########################
%#########################################################################

function [w_coh,phase]=wave_coher(x,y,wavelet,par,dt,alpha,J,scale)
%*************************************************************************
%This function calculates the Wavelet Squared Coherence.
%
%   INPUT:
%
%   x:          First time series to analyse.
%   y:          Second time series.
%   wavelet:    String variable defining the name of the wavelet function.
%               Possibilities are 'Morlet' or 'Paul'.
%   par:        Parameter defining the wavelet function. Used in the
%               anaylsis: par=6 for Morlet and par=4 for Paul wavelet.
%   dt:         Time step between each consecutive data point. (e.g. 1/12
%               for monthly data)
%   alpha:      Number of scales calculated between each consecutive power
%               of 2.
%   J:          Determines the maximum scale value, which will be
%               calculated.
%   scale:      Scale vector as defined above
%*************************************************************************
%Chapter 3.6:
%Wavelet Coherence
    cwt_pow_x = nag_cont_wtransform(x,wavelet,alpha,J,dt,par);
    cwt_pow_y = nag_cont_wtransform(y,wavelet,alpha,J,dt,par);

    cwt_cross = cwt_pow_x.*conj(cwt_pow_y);

%*************************************************************************
%Chapter 3.7:
%Calculation of the Phase Difference

    phase = atan( imag(cwt_cross)./real(cwt_cross) );

%*************************************************************************
%Chapter 3.6:

    cwt_pow_x = abs( cwt_pow_x ).^2;
    cwt_pow_y = abs( cwt_pow_y ).^2;

    for k=1:length(scale)
        norm = 1/scale(k);
        cwt_pow_x(k,:) = norm .* cwt_pow_x(k,:);
        cwt_pow_y(k,:) = norm .* cwt_pow_y(k,:);
        cwt_cross(k,:) = norm .* cwt_cross(k,:);
    end

%Smoothing the matrices in time
    cwt_pow_x = smooth_t(cwt_pow_x,wavelet, scale, dt);
    cwt_pow_y = smooth_t(cwt_pow_y, wavelet,scale, dt);
    cwt_cross = smooth_t(cwt_cross, wavelet,scale, dt);
```

```
    %Smoothing in scale
    cwt_pow_x = smooth_s(cwt_pow_x, wavelet,alpha);
    cwt_pow_y = smooth_s(cwt_pow_y, wavelet,alpha);
    cwt_cross = abs( smooth_s(cwt_cross, wavelet,alpha) ).^2;

    w_coh = cwt_cross ./ ( cwt_pow_x .* cwt_pow_y );

end

%*********************************************************************
%Smoothing is used from the wavelet toolbox from Grinsted, Moore and
%Jevrejeva (2004), but extended to Paul wavelets.

%#####################################################################
%###################### Time Smoothing ###############################
%#####################################################################

function [t_smoothed] = smooth_t(cwt,wavelet, scale, dt)

    t_smoothed = zeros(size(cwt));

    if ( strcmpi(wavelet, 'MORLET') )

    for o=1:length(scale)
        sc=scale(o)/dt;
        window_t=(-round(sc*3):round(sc*3))*dt;

        gauss = exp(- (window_t.^2)./ (2* scale(o)^2) );
        gauss_norm = gauss/sum(gauss);

        %Smoothing convolution as given in the main text. The smoothing
        %window has been normalised in the step before.
        t_smoothed(o,:)=conv(cwt(o,:),gauss_norm,'same');
    end

    elseif ( strcmpi(wavelet, 'PAUL') )
        for o=1:length(scale)
            m=4;
            sc=scale(o)/dt;
            window_t=(-round(sc*3):round(sc*3))*dt;

            window = (1+ (window_t.^2 ./ scale(o)^2)).^(-0.5*(m+1));
            window_norm = window/sum(window);

            %Smoothing convolution as given in the main text. The smoothing
            %window has been normalised in the step before.
            t_smoothed(o,:)=conv(cwt(o,:),window_norm,'same');
        end
    end

end




%#####################################################################
```

```
%####################### Scale Smoothing ###################################
%###########################################################################

function [s_smoothed] = smooth_s(t_smoothed,wavelet,alpha)

    if ( strcmpi(wavelet, 'MORLET') )
        decorrelation = 0.6;
    elseif ( strcmpi(wavelet, 'PAUL') )
        decorrelation = 1.5;
    end

    decorr_steps = decorrelation/(1/alpha*2);
    window_s=[mod(decorr_steps,1); ones(2 * round(decorr_steps)-1,1); ...
    mod(decorr_steps,1)]./(2*round(decorr_steps)-1+2*mod(decorr_steps,1));
    s_smoothed = conv2(t_smoothed,window_s,'same');

end

%References:
%
%   Torrence, C. and Compo, G.P. (1998). A practical Guide to Wavelet
%       Analysis, Bulletin of the American Meteorological Society, 79(1),
%       pp. 61-78.
%
%   Grinsted, A., Moore, J.C. and Jevrejeva, S. (2004). Application of the
%       cross wavelet transform and wavelet coherence to geophysical time
%       series. Nonlinear Processes in Geophysics, 11(5/6), pp.561-566.
%
%   The authors of both of the papers provide a Matlab toolbox, from which
%   ideas were taken at certain points. This code can be downloaded from
%   http://noc.ac.uk/using-science/crosswavelet-wavelet-coherence

%###########################################################################
%################################## End ####################################
%###########################################################################
```